

## Article

# Maturity Matters in Provenance Analysis: Mineralogical Differences Explained by Sediment Transport from Fennoscandian and Variscan Sources

Mette Olivarius \* , Henrik Vosgerau, Lars Henrik Nielsen, Rikke Weibel, Sebastian N. Malkki, Benjamin D. Heredia and Tonny B. Thomsen

Geological Survey of Denmark and Greenland (GEUS), Øster Voldgade 10, 1350 Copenhagen, Denmark

\* Correspondence: mol@geus.dk

**Abstract:** The significance of mineralogical maturity as a provenance indicator has long been debated and we use this study to demonstrate that it can indeed be a powerful tool to track the distribution of sandstone reservoirs. We investigate the cause of the pronounced geographic and stratigraphic differences in mineralogical composition that are found in the Upper Triassic–Lower Jurassic Gassum Formation across the Norwegian–Danish Basin and surrounding areas. Zircon U–Pb dating of 46 sandstone samples including analysis of 4816 detrital grains are combined with quantifications of the detrital mineralogical composition and placed in a sequence stratigraphic framework. The results show that the Gassum Formation can be divided into a southeastern region with high mineralogical maturity and a less mature region to the northwest with more feldspars, rock fragments, micas, and heavy minerals. Both the mineralogical assemblage and the provenance signature have been thoroughly homogenized in the SE region where sediment supplies from the Fennoscandian Shield and the Variscan Orogen are evident. In the NW region, sediment was initially supplied from Fennoscandia only, but the provenance abruptly changed from the Telemarkia Terrane to comprising also the more distant Caledonian Orogen resulting in a different mineralogical assemblage. The change occurred during a basinwide regression and may be caused by tectonic movements in the hinterland that permanently changed the composition of the sediment supplied to the basin.

**Keywords:** zircon U–Pb dating; sediment source areas; mineral assemblages; Variscan Orogen; Fennoscandian Shield; Gassum Formation



**Citation:** Olivarius, M.; Vosgerau, H.; Nielsen, L.H.; Weibel, R.; Malkki, S.N.; Heredia, B.D.; Thomsen, T.B. Maturity Matters in Provenance Analysis: Mineralogical Differences Explained by Sediment Transport from Fennoscandian and Variscan Sources. *Geosciences* **2022**, *12*, 308. <https://doi.org/10.3390/geosciences12080308>

Academic Editors: Andrew C. Morton, Shane Tyrrell, Gustavo Zvirtes and Jesus Martinez-Frias

Received: 30 June 2022

Accepted: 16 August 2022

Published: 18 August 2022

**Publisher's Note:** MDPI stays neutral with regard to jurisdictional claims in published maps and institutional affiliations.



**Copyright:** © 2022 by the authors. Licensee MDPI, Basel, Switzerland. This article is an open access article distributed under the terms and conditions of the Creative Commons Attribution (CC BY) license (<https://creativecommons.org/licenses/by/4.0/>).

## 1. Introduction

The term ‘mineralogical maturity’ is broadly used to describe the proportion between the most resilient minerals in the sedimentary cycle, such as quartz and zircon, relative to the less stable components, such as feldspars and rock fragments, that disintegrate more readily. A mineralogically mature quartz-rich sediment can be produced in several ways such as by chemical weathering, recycling of sediments, and diagenetic dissolution [1–4].

The detrital composition of the Upper Triassic–Lower Jurassic Gassum Formation sandstones varies considerably between the northwestern and southeastern parts of the Norwegian–Danish Basin [5]. Differences in diagenetic changes and hence in reservoir properties accompany these compositional variations. To improve the prediction of reservoir quality for undrilled parts of the Gassum Formation, it is crucial to achieving a better understanding of the provenance signal and how it differs, both spatially and temporally. The sandstones generally have high permeability at burial depths of c. 1–3 km [5,6]. However, strong control on the diagenesis and reservoir properties is exerted by the composition and maturity of the mineral assemblages, so obtaining knowledge of the provenance is of major importance. The provenance analysis presented here is therefore a key element in assessing the sediment transport routes, appointing sediment entry points to the basin,

understanding the depositional setting, explaining the large mineralogical variation, and thereby mapping the distribution and quality of the reservoir.

The Gassum Formation is the most widely distributed sandstone reservoir in the subsurface onshore and nearshore Denmark, where it is used for geothermal energy and storage of natural gas, besides having good potential for CO<sub>2</sub> storage and heat storage [7–16]. Knowledge of the trends in detrital mineralogical composition can help predict the diagenetic processes and thereby the permeability, along with the possible hydrogeochemical reactions that may occur in the sandstones during gas and CO<sub>2</sub> injection or geothermal production.

Zircon U-Pb dating has proven useful for the provenance analysis in this study, where a large dataset was obtained from wells across the region. Zircon is a heavy mineral that occurs in small amounts in most sandstones. Zircon grains are physically and chemically robust [17] so they can survive multiple episodes of deposition and reworking while still preserving the radiometric age of the crystalline rock in which it formed during an igneous or high temperature metamorphic event and from which it later eroded. This ability makes U-Pb dating of detrital zircon a unique provenance tool that is employed to trace the zircon grains in sedimentary rocks back to their original source area. Thus, zircon age information can give important insights into sediment transport routes, sediment distribution in the basin, and thereby also the depositional environments and paleogeography. There has been reported partial open system behavior in the U-Pb decay scheme for zircon and ancient Pb-loss at relatively low temperatures [18,19]. However, the high closure temperature of Pb in U-Pb zircon geochronology (>800 °C) allows all high temperature metamorphic or magmatic events in the region to be recorded.

The primary aim of the study is to contribute to the understanding of the governing processes for the reservoir properties of the Gassum Formation by analyzing evidence for source terranes. The formation contains many excellent reservoir sandstone units, but their distribution and quality are strongly dependent on the mineralogical composition and maturity in addition to the burial history. Previous studies have shown that the mineral assemblages were controlling the type of diagenetic alterations and resulting reservoir quality [5,20]. It is thus mandatory for reliable pre-drill predictions of reservoir properties that the source areas and the sediment transport routes are mapped to facilitate area specific predictions. By this means, we aim to illustrate the value of applying detrital zircon geochronology in source to sink analyses including paleogeographic reconstructions of basin development and changes in its hinterland and how it affects the detrital mineralogical composition.

## 2. Geological Setting

The Upper Triassic–Lower Jurassic Gassum Formation was initially defined in Denmark [21]. It was later redefined [22] and described in more detail [23,24]. The Gassum Formation occurs widespread in the Norwegian–Danish Basin, which was formed during regional subsidence following rifting phases [25]. The basin is separated from the North German Basin by the Ringkøbing–Fyn High comprising shallow basement crosscutting the southern part of the Danish area (Figure 1). The Gassum Formation is only preserved locally on and south of the Ringkøbing–Fyn High along the northern flank of the North German Basin since the sediments were deeply eroded during the Middle Jurassic when the high and parts of the surrounding basins were uplifted [24].

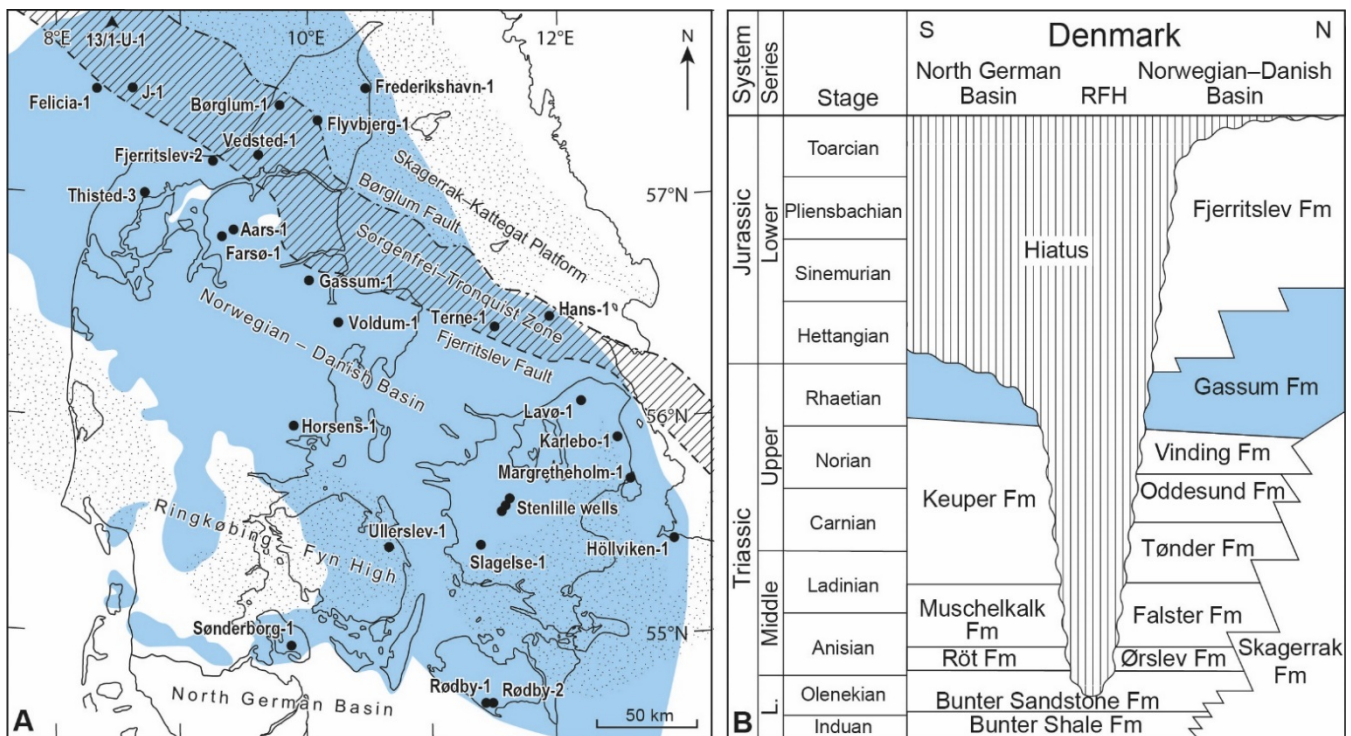


**Figure 1.** (A) Map showing structural elements and wells used in this study and with the estimated distribution of the Gassum Formation in the Danish area shown in blue. Modified from [5]. (B) Stratigraphic scheme of the Lower Triassic to Lower Jurassic succession onshore Denmark that is based on [24,26]. The time-transgressive nature of the top of the Gassum Formation is indicated. The Norwegian–Danish Basin and the North German Basin were separated by the Ringkøbing–Fyn High (RFH) on which less sediments were deposited, of which some were later eroded.

The thickness and depth of the Gassum Formation vary considerably across Denmark due to different depositional regimes and burial histories [24,27], which has resulted in variable reservoir quality [5]. The formation has thicknesses of mostly 50 to 300 m and is thicker locally, for example in the Sorgenfrei–Tornquist Zone [12,13,23,24]. The largest depths of the formation of >3 km occur in the basin centre in central Jylland and the smallest depths of <1 km are found near the basin margins to the north and along the northern and southern margins of the Ringkøbing–Fyn High. The formation was deposited in a humid climate during repeated sea-level fluctuations and comprises fluvial, estuarine, and shoreface sandstones interbedded with marine, lagoonal and lacustrine mudstones, and siltstones [24].

Two basement provinces occur sufficiently close to the Danish area to constitute possible sediment source areas, namely the Fennoscandian Shield to the north and the Variscan Orogen to the south (Figure 2). The southern part of the Fennoscandian Shield comprises the Sveconorwegian Orogen in southern Norway and southwestern Sweden consisting of the Telemarkia Terrane, the Idefjorden Terrane, and the Eastern Segment that formed at 1.52–1.48 Ga, 1.66–1.52 Ga and 1.80–1.64 Ga, respectively [28]. Intrusions formed at 1.47–0.91 Ga and metamorphism occurred at 1.14–0.90 Ga, which was most pronounced in the Telemarkia Terrane [29]. The Caledonian Orogen covers central southern Norway and further north. It includes the Lower and Middle Allochthons in which most ages are 1.69–1.62 Ga corresponding to the basement windows in southern Norway, whereas magmatic (Caledonian) ages of 0.50–0.42 Ga are present in the Upper and Uppermost Allochthons [28]. Magmatism at 0.30–0.28 Ga resulted in the extrusion of lavas in the Oslo Graben [30]. The Variscan belt is comprised primarily of rocks of the Cadomian and Variscan orogeneses, formed at 0.65–0.28 Ga [31,32].

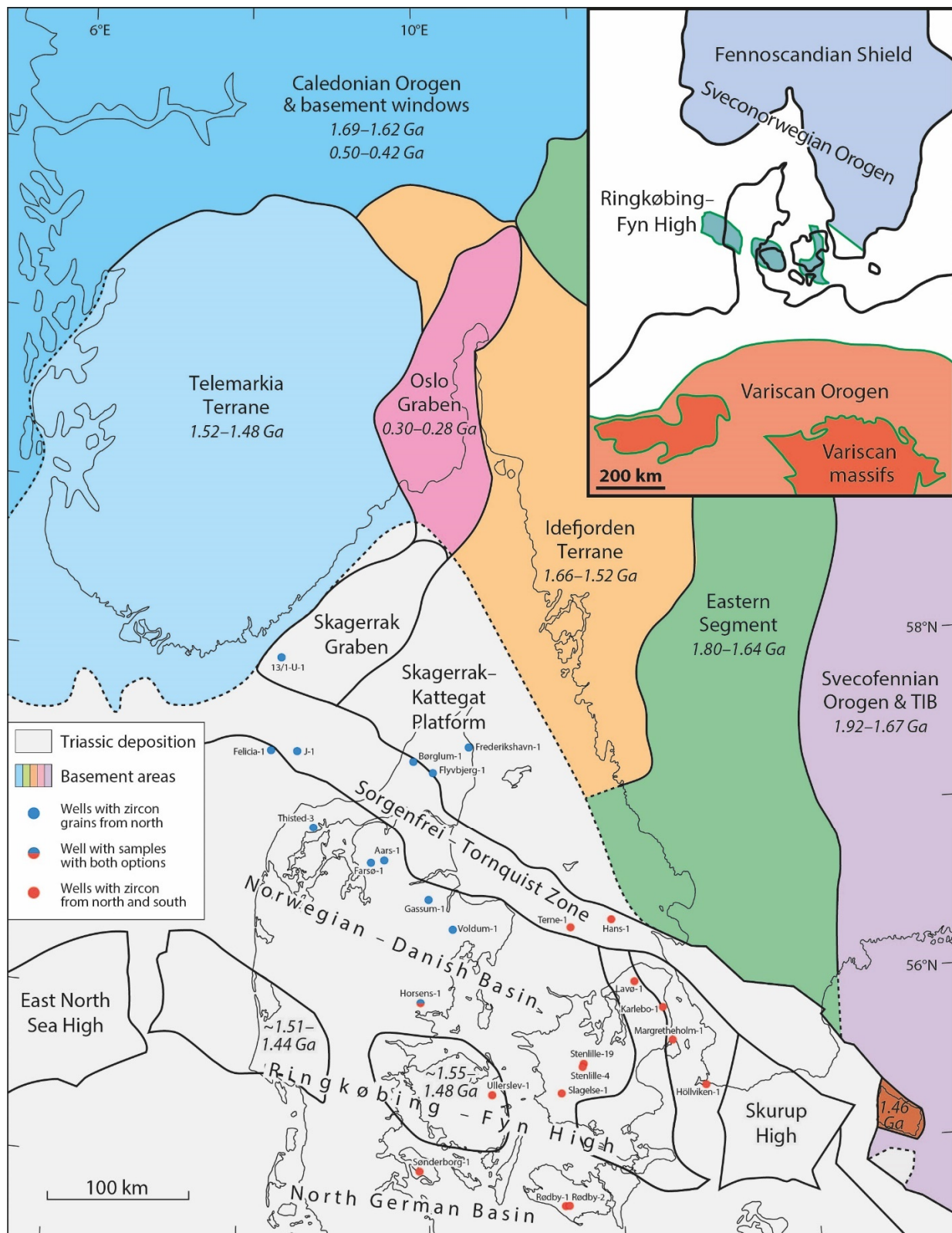


**Figure 2.** Map of the basement provinces in the southern part of the Fennoscandian Shield with indications of their magmatic zircon ages. The location of the Variscan Orogen is outlined on the overview map. The wells show where zircon U-Pb analyses of the Gassum Formation were made. TIB: Transscandinavian Igneous Belt. The area of Triassic deposition is based on [13,33,34]. The structural elements are from [24,28,30,35,36]. The ages in billion years (Ga) are from [28,37–39].

### 3. Samples

Samples from the Gassum Formation were collected from sandstones in cores and from sandy intervals in cuttings samples from 25 selected wells (Figure 2). The sample selection focused on (1) covering the large geographical area, (2) covering the stratigraphic variation, and (3) deciphering the mineralogical difference observed in the northwestern versus southeastern part of the Gassum Formation. Zircon grains from 46 samples were analyzed, of which 24 of the samples are from the northwestern part of the study area i.e., from the wells 13/1-U-1, Felicia-1, J-1, Frederikshavn-1, Flyvbjerg-1, Børglum-1, Thisted-3, Farsø-1, Aars-1, Gassum-1, Voldum-1, and Horsens-1, and 22 of the samples are from the southeastern part of the study area i.e., from the wells Terne-1, Hans-1, Lavø-1, Karlebo-1, Margretheholm-1, Höllviken-1, Stenlille-4, Stenlille-19, Slagelse-1, Ullerslev-1, Rødby-1, Rødby-2, and Sønderborg-1. The results from the 5 samples from the 13/1-U-1, Felicia-1, and J-1 wells were presented by [40].

The depths of the core samples represent the average depth of the sampled interval, which is up to 10 cm thick, except for samples from the 13/1-U-1 and Höllviken-1 wells where limited material was available. Here the intervals are larger. Cores from the Gassum Formation are scarce in the offshore areas and in the southeastern part of the study area, so some of the samples were obtained from cuttings. The sampled intervals of the cuttings samples are from 1.5 to 18 m thick to ensure that sufficient material was collected (c. 300 g). The depths represent those measured in the wells (MD). However, in some wells, the core depths do not correspond exactly to the well log depths, so correction is required when comparing samples with well logs [24].

Many surfaces in the Gassum Formation can be correlated across the Danish area by means of stratigraphic sequences, and the NW–SE oriented correlation panel in Figure 3 shows that thick sandstone beds are present at both ends of the basin. The basinwide regression causing the formation of sequence boundary 5 (SB 5) is evident by the overlying basinwide estuarine and fluvial deposits. In this study, the section below SB 5 is referred to as the lower part of the Gassum Formation, and the section above is the upper part. The overall backstepping of the basin margins during the earliest Jurassic deposition is evident by the uppermost sandstone layers only being present towards the north. Only the upper part of the Gassum Formation is present in the Frederikshavn-1, Flyvbjerg-1, and Børglum-1 wells [24], so just one sample has been analyzed from each of these wells.

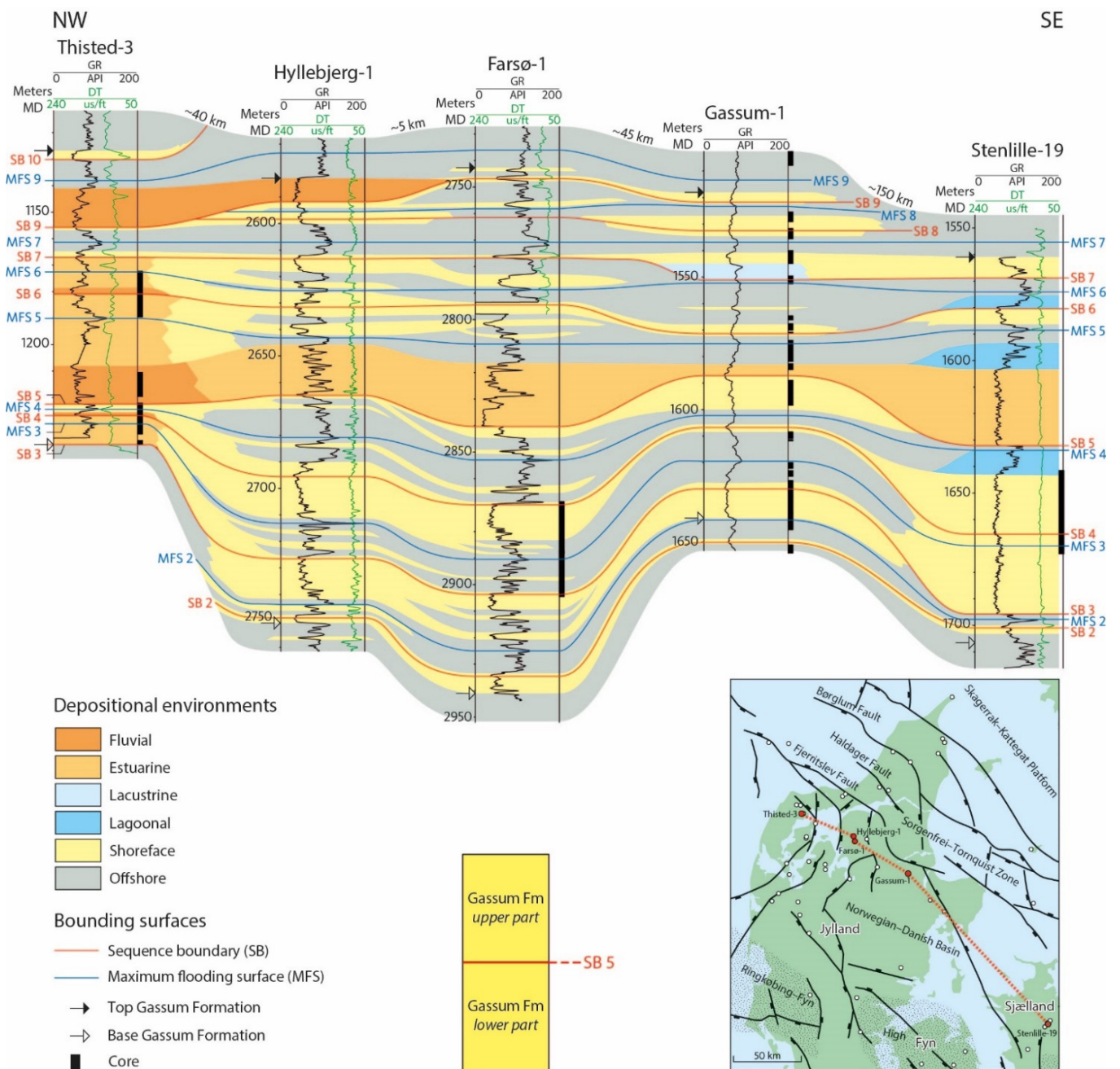


**Figure 3.** Wireline logs of Gassum Formation from five wells in the Norwegian-Danish Basin with interpreted depositional environments, sequence stratigraphic boundaries and correlations between wells. The stratigraphic framework is based on [24]. The basinwide regression at SB 5 marks a change in zircon U-Pb ages and sediment composition in Jylland but not in Sjælland.

#### 4. Methods

Zircon U-Pb geochronological analysis was carried out at GEUS on a total of 4816 grains. The cuttings samples were washed to remove drilling mud. All samples were crushed and sieved to extract zircon grains from the 45–750 μm grain size fraction. The zircon grains were handpicked from heavy mineral concentrates obtained by density sorting using a Holman-Wilfley water-shaking table, and then embedded in epoxy, imaged, and checked by scanning electron microscopy (SEM) where cathodoluminescence (CL) images were obtained. Zircon grains of all available sizes, morphologies, and colors were selected for analysis. The location for analysis within each grain was selected based on the internal

texture according to the CL information, where inclusions and cracks were avoided. The grains were analyzed in magmatic zircon with oscillatory zoning, either in the core of the grains or in homogeneous zoning if the core was not homogeneous (Figure 4). The zircon grains were analyzed by laser ablation inductively coupled plasma mass spectrometry (LA-ICPMS), using an NWR 213 laser ablation instrument coupled to an Element2 magnetic sector-field ICPMS.

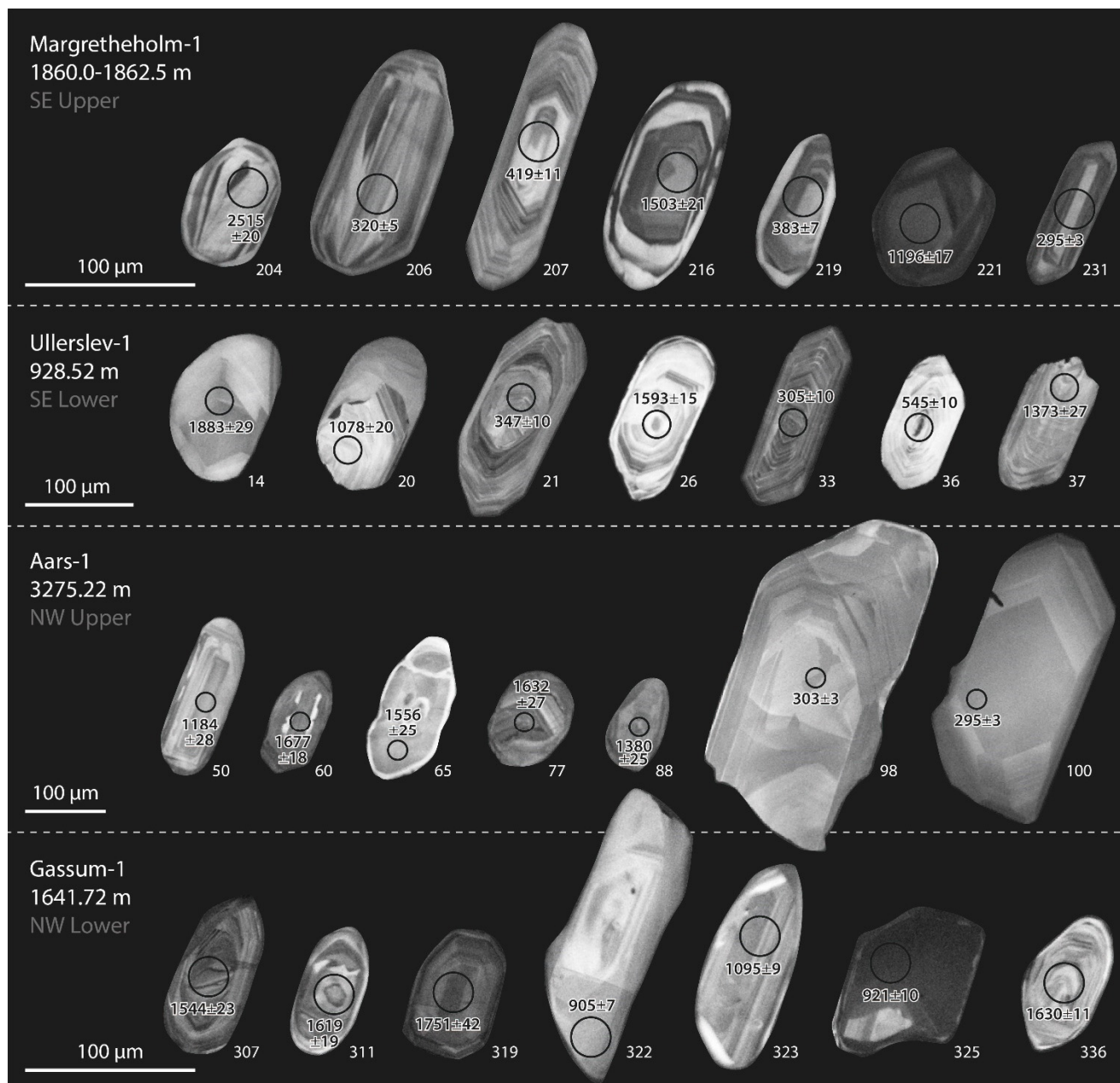


**Figure 4.** Cathodoluminescence images showing typologies and internal texture of representative zircon grains from selected samples including one from each of the NW Lower, NW Upper, SE Lower, and SE Upper regions. The analysis spots and U-Pb dates (Ma) are indicated, along with the spot numbers.

The zircon grains were ablated for 30 s in an air-tight helium-flushed chamber using a focused laser beam with a diameter of 25 or 30 micrometres (μm), a repetition rate of 10 Hz, and an output energy density of c. 10 J/cm<sup>2</sup>. The liberated material was transported through inert Tygon tubing by the helium carrier gas to the mass spectrometer

for isotopic determination. To minimize instrumental drift, a standard-sample-standard analysis protocol was followed, bracketing the zircon analyses by measurement of the zircon standard GJ-1 [41]. For quality control, secondary zircon standards were used, i.e., Plešovice [42] and for the newer analyses also Harvard 91500 [43,44], both yielding an average age accuracy and precision ( $2\sigma$ ) within 3% deviation.

Data reduction was performed using the Iolite v2.5 software and the in-house software Zirchron [45–47]. Combined histogram and probability-density plots were produced through the software jAgeDisplay [48]. The discordance of the analyses was calculated according to the Wetherill Concordia [49] and the relative age difference between the  $^{206}\text{Pb}/^{238}\text{U}$  and  $^{207}\text{Pb}/^{206}\text{Pb}$  ages (e.g., [50]). Based on adjustment of the concordance threshold, it was chosen only to plot dates within  $\pm 10\%$  discordance interval since higher discordance relates to inadequate data quality or complexity (in terms of understanding metamict zircon due to partial Pb-loss from processes like alpha-recoil, diffusion, leaching, recrystallisation, residence time, etc.), which distorts the age distributions.

The  $^{206}\text{Pb}/^{238}\text{U}$  dates represent the direct dates from the counting statistics in the mass spectrometer and these are plotted for the data up to a certain crossover date. The derived  $^{207}\text{Pb}/^{206}\text{Pb}$  dates are better suited for the older zircon grains as the excess variance is reduced due to more precise measurements of the (larger) ion beams signals for the  $^{207}\text{Pb}/^{206}\text{Pb}$  ratio. Based on fine-tuning of the crossover between  $^{206}\text{Pb}/^{238}\text{U}$  and  $^{207}\text{Pb}/^{206}\text{Pb}$  dates, it is chosen to use a crossover age at 1200 Ma primarily based on the lowest possible uncertainties ( $2\sigma$ ) of the dataset. The estimation of a crossover age is in part instrument-specific, so the plotted zircon age distributions are comparable to those plotted with other crossover ages.

A common-lead correction was applied to a subset of the analyses when required, including a total of 447 grains. The correction was made using measured mass 204 (i.e.,  $^{204}\text{Hg} + ^{204}\text{Pb}$ ) corrected for Hg through the  $^{202}\text{Hg}/^{204}\text{Hg}$  natural abundance ratio. Skewing of some of the age populations towards younger dates were found for the common-lead corrected data when comparing them with the remaining age data, thus the corrected data were excluded. According to [18], age displacement may happen because old Pb-loss can be hidden by younger Pb-loss such that the common-Pb correction of grains that have experienced several episodes of Pb-loss produces a date that is younger than the true value.

The detrital mineralogical composition of the Gassum Formation was studied by optical microscopy and SEM and quantified by point counting in thin sections of 93 sandstone samples. Some of these data have been presented by [5,20]. Mineral maps of selected thin sections were produced at GEUS by the automated quantitative mineralogy method (AQM) as described by [51] on a Zeiss Sigma 300VP SEM with a back-scattered electron (BSE) detector and two Bruker XFlash 6|30 EDX 129 eV detectors using the Zeiss Mineralogic software platform.

## 5. Results

The results of the zircon U-Pb dating of the Gassum Formation are available in the Supplementary Material. The data are plotted as age distributions for each sample in Figure 5 divided into the northwestern part (Skagerrak and Jylland; Figure 5A) and the southeastern part of the study area (Kattegat, Sjælland, Amager, Skåne, Lolland, Fyn, and Als; Figure 5B). Furthermore, the samples are plotted in four groups comprising the NW Lower, NW Upper, SE Lower, and SE Upper parts of the formation (Figure 6), where the split between lower and upper is at the regional sequence stratigraphic surface SB 5 defined by [24].



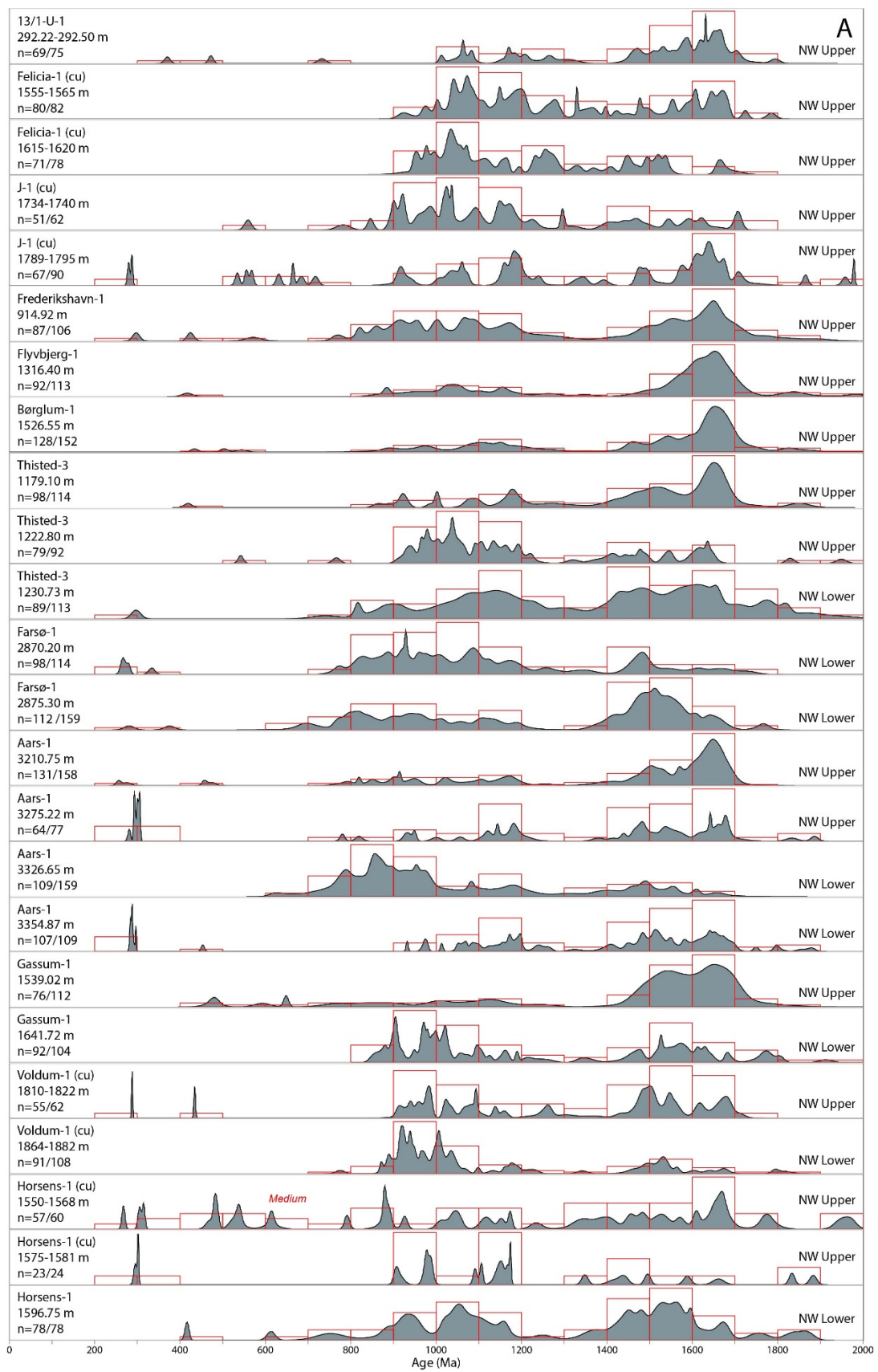
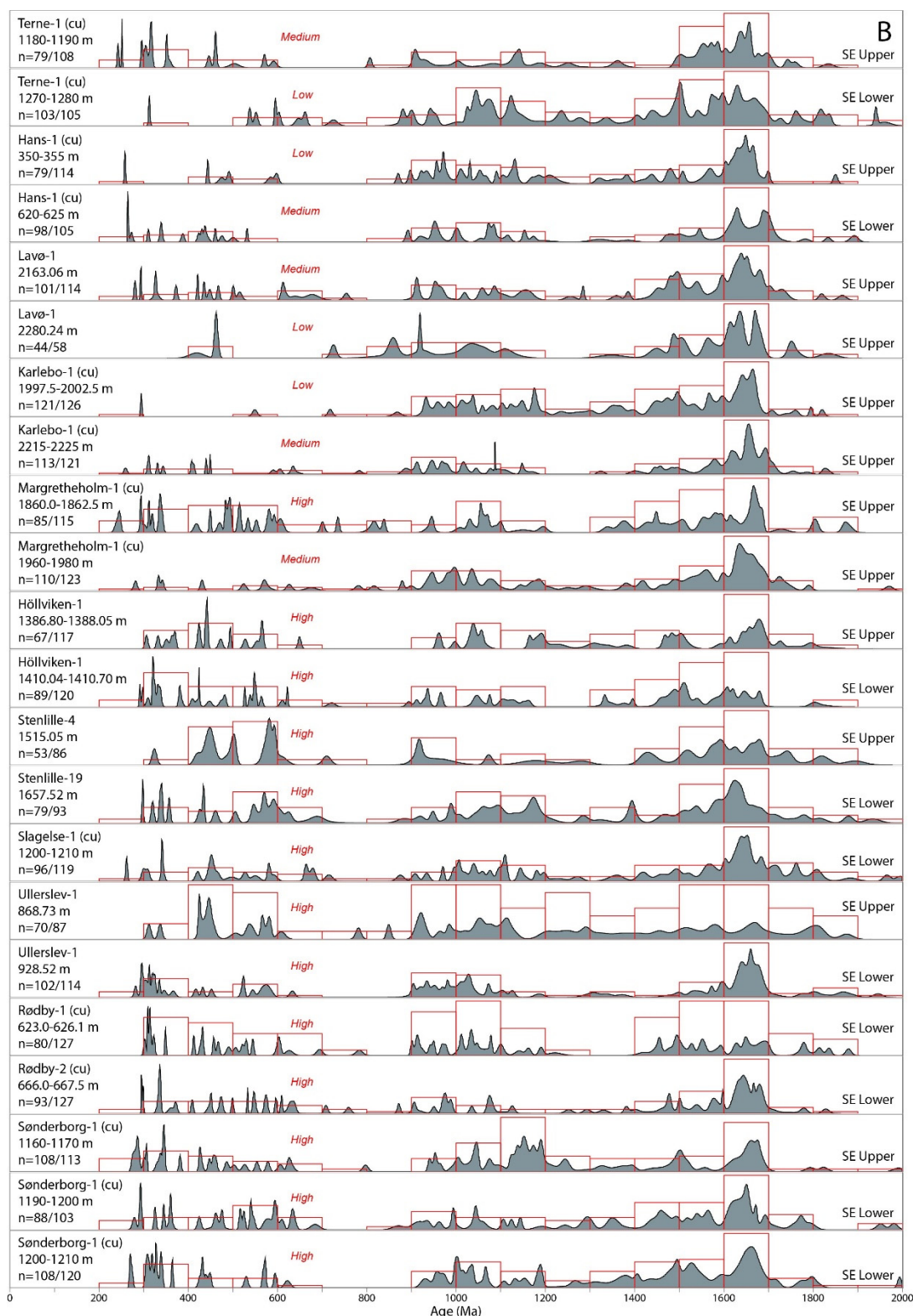
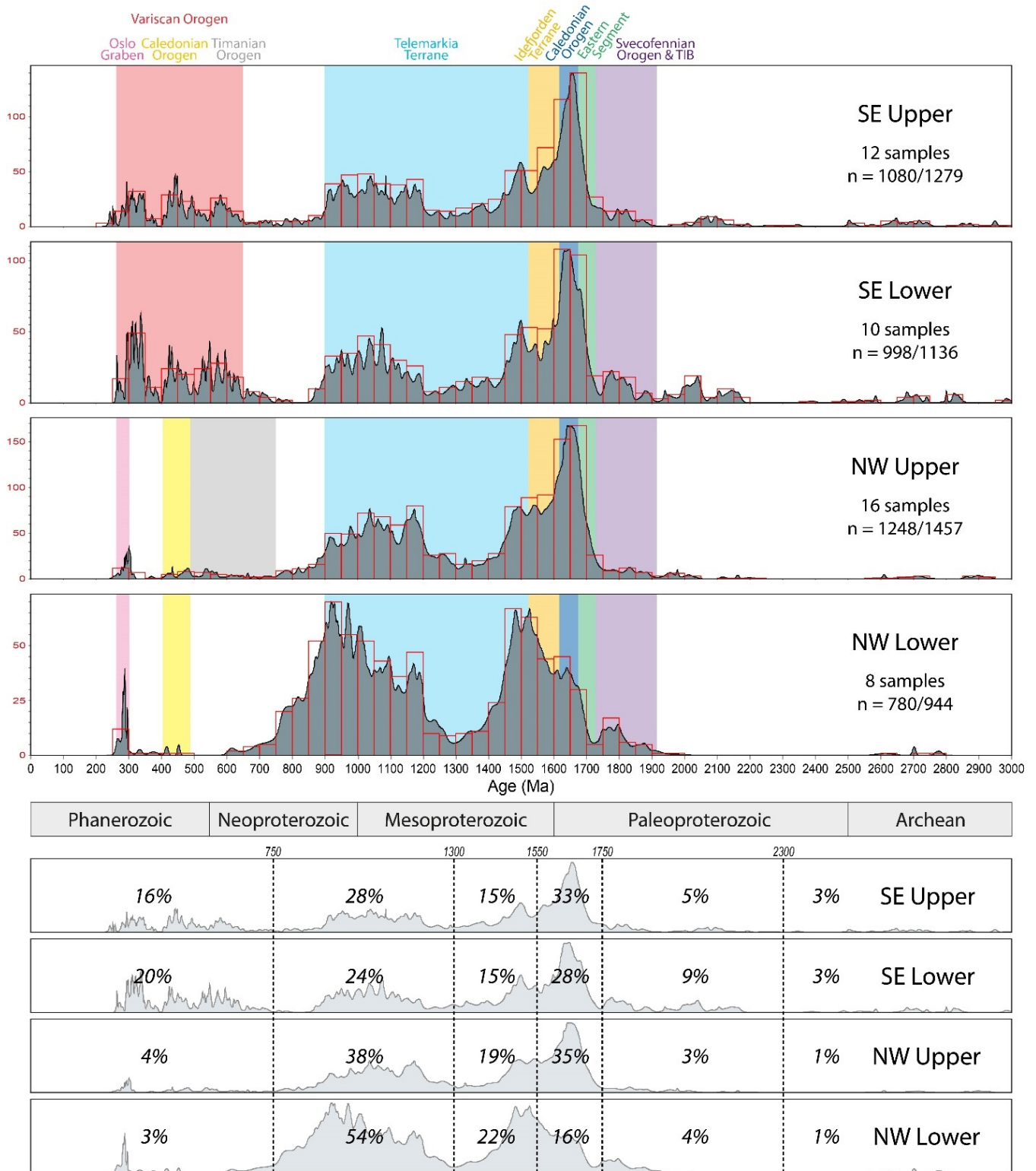


Figure 5. Cont.



**Figure 5.** Zircon U-Pb age distributions with 100 Ma histograms for the northwestern (A) and southeastern (B) parts of the Gassum Formation. The well name, depth and number of concordant zircon age analyses are shown for each sample. Only ages with a discordance < 10% are included, and results with common lead are excluded. A crossover age at 1200 Ma between  $^{206}\text{Pb}/^{238}\text{U}$  and  $^{207}\text{Pb}/^{206}\text{Pb}$  dates is applied. A qualitative estimate of the relative amount of Variscan ages in the samples is indicated as high/medium/low. Most samples are from cores, whereas some are from cuttings (cu).



**Figure 6.** Zircon U-Pb age distributions with 50 Ma histograms. Samples are merged for the NW and SE parts of Gassum Formation divided into the lower and upper part. Ages with a discordance < 10% and without common lead are included. The most likely origins of the zircon age populations are visualized by colors (see Figure 2 for locations of the basement areas). The relative proportions of the number of ages within six age intervals are shown by percentages.

The age distributions reveal that the zircon grains in all 46 samples are primarily derived from the Fennoscandian Shield as seen by the multiple age populations present in the 1.8–0.9 Ga age interval (Figure 5). Fennoscandian zircon dates younger than this are restricted to Paleozoic ages corresponding to the Ordovician to Early Devonian Caledonian orogeny and the Late Carboniferous to Permian Oslo rifting. These fall within age ranges of 0.50–0.42 and 0.30–0.28 Ga, respectively, which overlap with the age range of 0.65–0.28 Ga that characterize the Variscan Orogen. The small contents of young zircon grains from the Caledonian Orogen and Oslo Graben found in some of the samples from the northwestern part of the Gassum Formation can be clearly distinguished by their narrow age ranges (Figure 5A) as compared to the multiple age populations from the Variscan Orogen present in the samples from the southeastern part of the formation (Figure 5B). It is not possible to recognize if small contents of young zircon grains from Fennoscandia are present in the southeastern part of the Gassum Formation since such ages would be masked by the larger content of zircon grains from the Variscan Orogen. However, zircon grains from the Oslo Graben can have much larger sizes (Figure 4, Aars-1, 3275.22 m).

In samples from the northwestern part of the study area, the content of Caledonian-aged zircon grains is very small, when present, constituting no more than 1–2 grains, whereas the content of zircon grains from Oslo Graben in some cases is higher such as in two of the samples from the Aars-1 well (Figure 5A). No pattern is evident in the geographical distribution of the young zircon grains of Fennoscandian affinity in the Gassum Formation. In the lower sample from the J-1 well, ages corresponding to the Timanian Orogen of 0.75–0.49 Ga are found [40].

A qualitative estimate of the relative amount of Variscan ages found in the samples has been made where “high” refers to a significant Variscan sediment input, “medium” refers to a clear but moderate input, and “low” refers to a small indistinct input (Figure 5). High Variscan input is found in all samples from the Höllviken-1, Stenlille-4, Stenlille-19, Slagelse-1, Ullerslev-1, Rødby-1, Rødby-2, and Sønderborg-1 wells. High Variscan input is also found in one of the samples from the Margretheholm-1 well, whereas the other sample from this well has a medium Variscan input. From each of the Terne-1, Hans-1, Lavø-1, and Karlebo-1 wells are analyzed two samples of which one has medium and the other has low Variscan input, but without a consistent stratigraphic trend. Medium Variscan input is found in the upper sample from the Horsens-1 well, whereas the other samples from this well show no Variscan input. Variscan ages are neither identified in the remaining samples from the northwestern part of the Gassum Formation, although it cannot be excluded that a few Variscan zircon grains may be present in some samples (Figure 5). Except for the geographical variations found in the abundance of Variscan ages, the age distributions from the southeastern part of the Gassum Formation are very uniform (Figure 5B). A dominance of c. 1.65 Ga dates is found in all histograms, which corresponds to the old zircon ages in the Caledonian Orogen, since such ages are not prominent in the Sveconorwegian Orogen—although they do exist in the Idefjorden Terrane and the Eastern Segment. In the Sønderborg-1 well, a content of angular rock fragments besides quartz grains with rounded overgrowths points to local erosion of the basement and possibly cover sediments in the Ringkøbing–Fyn High.

The multiple age populations present in the 1.8–0.9 Ga age interval in the northwestern part of the Gassum Formation correspond to the ages that occur in the Sveconorwegian Orogen, including intrusions and metamorphic overprint (Figure 5A) of which the youngest ages are often in the rim of the grains (Figure 4, Gassum-1, 1641.72 m). A local provenance is evident from the high content of zircon grains with ages corresponding to the metamorphic events that were most pronounced in the Telemarkia Terrane in southernmost Norway. This is therefore the likely provenance of most of the sediment in the northwestern part of the study area. However, the Caledonian Orogen is the primary source area of the uppermost samples from the Frederikshavn-1, Flyvbjerg-1, Børglum-1, Thisted-3, Aars-1, Gassum-1, and Horsens-1 wells, which have age distributions that resemble those from southeastern Denmark with the dominance of c. 1.65 Ga ages, except that samples from

northwestern Denmark do not contain Variscan zircon grains apart for the uppermost sample from Horsens-1 (Figures 5 and 6).

When comparing the merged age distributions, it is evident that the SE Lower and SE Upper groups are comparable, and that the distribution of Fennoscandian ages in the NW Upper group is more similar to the SE groups than to the NW Lower group (Figure 6). The relative proportion of zircon grains with ages younger than 750 Ma is 20 and 16% in the SE Lower and SE Upper groups, respectively. It is 3 and 4% in the NW Lower and NW Upper groups, so the content of young zircon grains is the most marked difference between the overall SE and NW areas.

The detrital mineralogical composition of the Gassum Formation sandstones is presented in Table 1. The results are grouped according to the southeastern versus northwestern part of the study area and the lower versus upper part of the formation. The mineralogical composition is comparable for SE Lower and SE Upper groups that have average quartz contents of 91 and 92%, respectively. Furthermore, they contain 5% K-feldspar and 2% plagioclase, besides small contents of rock fragments, mica minerals, and heavy minerals, and they are mostly very well to extremely well sorted. Quartz grains with rounded overgrowths were observed in some samples from the SE groups, though not in samples from the NW groups. Some of the rounded quartz overgrowths are enclosing red coatings consisting of Fe-oxides/hydroxides formed in an arid climate (Figure 7).

**Table 1.** Mineralogical composition of detrital grains in the Gassum Formation based on petrographic point counting. The southeastern part of the formation is better sorted and contains more quartz than the northwestern part of the formation, which has much higher contents of most other types of grains. Some clear differences are evident between the lower and upper intervals of the northwestern part of the formation. SB 5 marks the boundary between the lower and upper intervals of the Gassum Formation. Data from the southeastern part of the Gassum Formation are from the Margrethholm-1, Stenlille-1, -5, -15, -18, and -19 wells, and data from the northeastern part are from the Aars-1, Børglum-1, Farsø-1, Fjerritslev-2, Flyvbjerg-1, Gassum-1, Thisted-3, and Vedsted-1 wells. Each column has been formatted with a separate color scale from highest (green) to lowest (white) values.

NW vs SE and Upper vs Lower Part of Gassum Formation	Number of Samples	Mean Grain Size (mm)	Sorting (Trask P75/P25)	Quartz Grains (Monocrystalline)	Quartz Grains (Polycrystalline)	K-Feldspar Grains	Plagioclase Grains	Carbonate Grains	Glauconite Grains	Sedimentary Rock Fragments	Plutonic Rock Fragments	Volcanic Rock Fragments	Metamorphic Rock Fragments	Muscovite Grains	Biotite Grains	Chlorite Grains	Heavy Mineral Grains
SE Upper	11	0.22	1.25	87.13	4.78	4.84	1.53	0.00	0.00	0.70	0.25	0.00	0.17	0.22	0.00	0.00	0.39
SE Lower	10	0.25	1.50	84.34	6.77	5.24	1.56	0.00	0.00	0.43	0.56	0.09	0.00	0.38	0.00	0.00	0.64
NW Upper	43	0.27	1.98	63.22	9.35	8.84	9.55	0.05	0.33	0.72	1.38	0.20	0.96	2.69	1.26	0.34	1.12
NW Lower	29	0.27	1.95	56.60	7.25	9.12	19.57	0.25	0.54	0.51	1.68	0.05	0.47	0.60	1.86	0.02	1.48

The sandstones from the northwestern part of the formation are mostly more poorly sorted and have a slightly larger average grain size than those from the southeast. The NW Lower group contains 64% quartz, 9% K-feldspar, and 20% plagioclase, whereas the NW Upper group has 73% quartz, 9% K-feldspar, and 10% plagioclase. The NW Lower and Upper groups contain more polycrystalline quartz, rock fragments, mica minerals, and heavy minerals than the SE Lower and Upper groups, though the proportion varies much between the NW groups (Table 1). Mineral maps from the NW Lower group from the Gassum-1 well and from the SE Upper group from the Stenlille-15 well are shown as examples to illustrate the large regional mineralogical difference (Figure 8). The sandstones from both these wells have been buried c. 600 m deeper

prior to the Neogene uplift [27,52]. The wells in which the mineralogical composition was studied are shown on the map where the mineralogical maturity regions are outlined and which comprise the low maturity region to the NW with high content of feldspars, among others, and the high maturity region to the SE with abundant quartz.

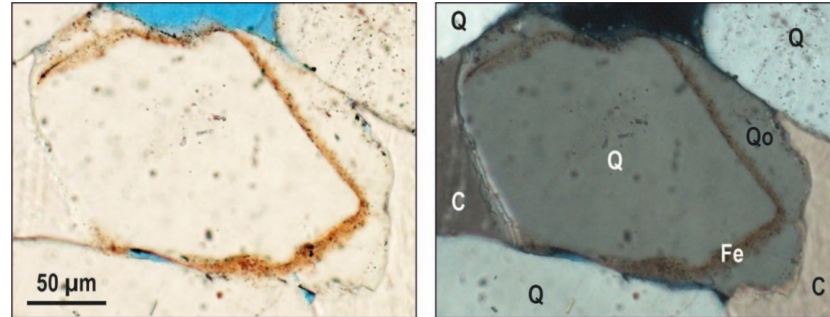


**Figure 7.** Quartz grain (Q) with Fe-oxide/hydroxide coating (Fe) and rounded quartz overgrowth (Qo) embedded in carbonate cement (C). The red coating must have formed in an arid depositional environment and have been overgrown by quartz before being eroded and reworked into the Gassum Formation. Sandstone from the Stenlille-15 well at 1599.50 m. Crossed nicols to the right.

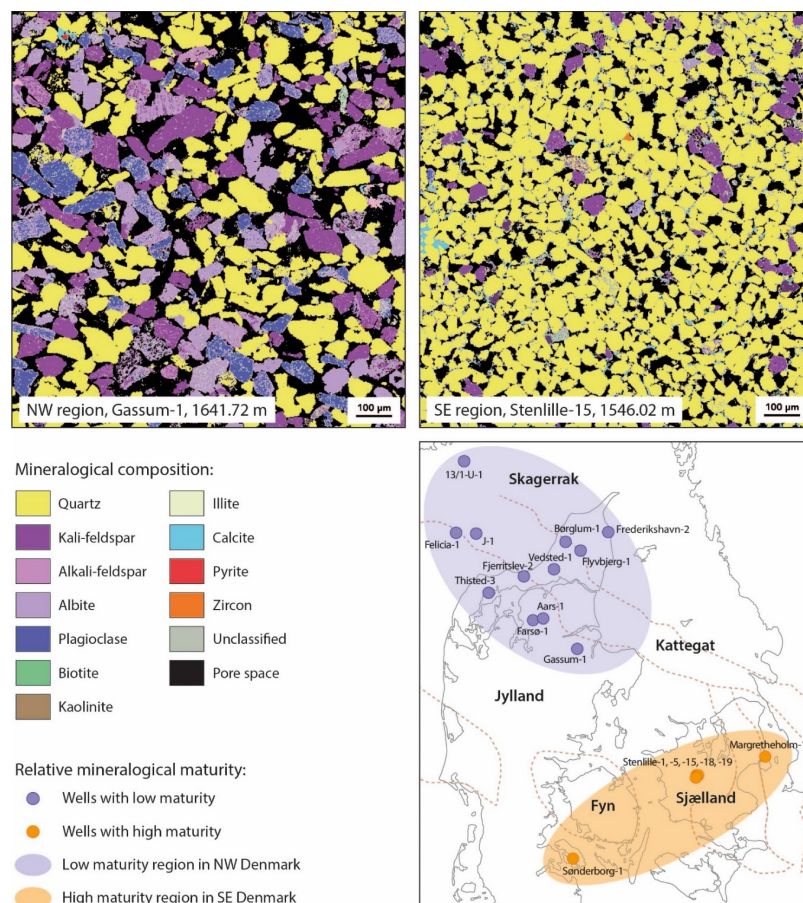


**Figure 8.** The mineralogical maturity of the Gassum Formation varies across the Danish area. The AQM mineral maps of two sandstone samples show the mature mineralogical composition on Sjælland with high quartz content, whereas a less mature composition with higher contents of especially feldspars is found in Jylland. The map shows where the mineralogical composition of the Gassum Formation has been examined. Based on this information, the formation can be divided into regions with relatively high versus low mineralogical maturity.

## 6. Discussion

A Fennoscandian provenance of the Gassum Formation has long been assumed merely from facies distribution and the geometry of the depositional units in the basin [53]. This is now confirmed by the provenance analysis of detrital zircon grains, and the present data furthermore identify a significant additional sediment input with Variscan affinity (Figure 6).

A Paleozoic sediment cover once existed in southwestern Sweden [54]. This cover was mostly removed during the Middle Triassic uplift [55] by which time the area had been peneplained and did therefore not supply much sediment to the Gassum Formation since the peneplain consisted mostly of resilient basement. Some Paleozoic sediments are locally preserved in the Sveconorwegian Orogen in down-faulted areas such as the Oslo Graben [56–58]. A small sediment supply from the Oslo Graben is identified in a few samples based on Carboniferous–Permian zircon ages corresponding to the timing of the rifting (Figures 5 and 6). Sediments constituted probably only a minor part of the exposed rocks in the Fennoscandian Shield when the Gassum Formation was deposited, meaning that the sediment supplied from the north is primarily derived from erosion of basement terranes without significant reworking of sedimentary rocks. This is also reflected in the relatively low mineralogical maturity of the sediment supplied from the north.

The zircon grains with ages of 0.75–0.49 Ga found in the J-1 well (Figure 5A) are rare in southern Fennoscandia since they originate from the Timanian Orogen that is located northeast of the shield. However, it was eroded during the Cambrian–Ordovician and some of the detritus was deposited in southern Norway where it is locally preserved [59], and some of it has been reworked into the Gassum Formation [40].

In the northwestern part of the Gassum Formation, the highly varying proportion of the individual zircon age populations indicates a local provenance where limited homogenization of the provenance signal has occurred along the short sediment transport pathways (Figure 5A). The opposite is found in the southeastern part of the formation as evident by the uniform age distributions, implying intensive homogenization and mixing of sediment from several source areas (Figure 5B). This trend is well illustrated in Figure 9 where the homogeneity of the SE groups is evident, in the sense that the distribution of ages and relative abundance of age populations are comparable between the samples. The individual samples in the NW groups show larger variation in their age distributions so they are less comparable showing that less mixing of sediment supplies from the different source areas has occurred.

Most of the sediment in the northwestern part of the Gassum Formation was only transported a short distance from its source area, the Telemarkia Terrane in southernmost Norway, which is in accordance with the low mineralogical maturity presumably reflecting short fluvial transport (Figure 8). The plagioclase content is halved in the NW Upper group compared to the NW Lower group (Table 1). This is in accordance with the longer sediment transport route from the Caledonian Orogen in central southern Norway interpreted as the primary source of the upper part of the formation in this area, which could have caused more breakdown of feldspars and in particular of plagioclase than in the lower part of the formation, since plagioclase is more sensitive to weathering than K-feldspar [60]. The sediment was probably transported in large meandering rivers, with temporary storage along the route allowing time for intensive chemical weathering in the humid climate. The increased content of metamorphic rock fragments and muscovite in the NW Upper group compared to the NW Lower group also shows that different types of rocks were supplying the sediment since the Caledonian nappes comprise primarily metasedimentary rocks. This change may be related to the general backstepping of the basin edge due to the marine drowning that culminated with the deposition of the Fjerritslev Formation [24], or it could be related to a changed topography of the source area. However, in Skagerrak, sediment was continuously supplied from the Telemarkia Terrane to the Gassum Formation so a change in provenance did not occur closest to this source area.

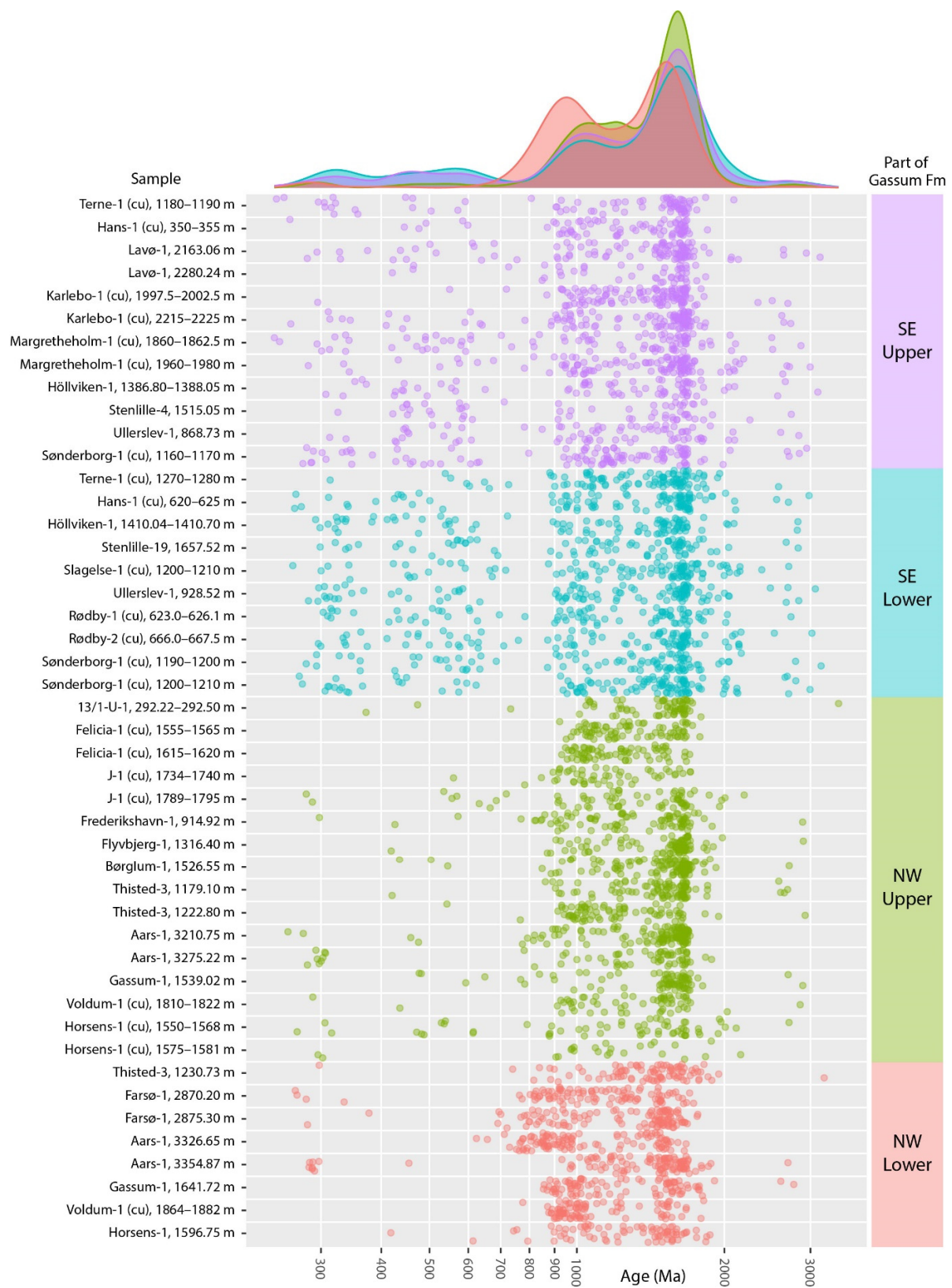


**Figure 9.** Plot of  $^{206}\text{Pb}/^{238}\text{Pb}$  and  $^{207}\text{Pb}/^{206}\text{Pb}$  zircon data with crossover at 1200 Ma plotted for all samples on a logarithmic scale. The samples are grouped into the NW and SE part of Gassum Formation, and into the lower and upper part (divided by sequence boundary 5). The probability density distributions at the top show the merged age distribution for each of these groups. Most samples are from cores, and some are from cuttings (cu).



Most of the sediment in the southeastern part of the Gassum Formation was transported a long distance from the Caledonian Orogen, and some Sveconorwegian sediment has been added to the detritus in the fluvial system when passing through this area. Especially from the Telemarkia Terrane, whereas zircon dates corresponding to the broad spectrum of ages present in the Idefjorden Terrane and the Eastern Segment are not prominent in the Gassum Formation (Figures 5B and 6). The southeastern part of the Gassum Formation is positioned further away from the Caledonian Orogen than the northwestern part (Figure 2), which is part of the explanation for the lower feldspar content in the southeastern part (Table 1). The sediment supplied from the Variscan Orogen to the southeastern part of the Gassum Formation was also transported a long distance before deposition. Intensive weathering during temporary storage along the transport route is a more likely cause than repeated reworking of the high mineralogical maturity present in the southeast since there are no major variations in feldspar abundances between fluvial and shoreface sandstones [5]. Reworking of older sedimentary rocks from the south has also contributed to the high mineralogical maturity as seen by the presence of rounded quartz overgrowths enclosing red coatings (Figure 7), which are not seen in the northeastern part of the Gassum Formation. The composition of the sediment source rocks is also of importance, where smaller proportions of feldspars are characteristic of sediments sourced from the south.

The Bunter Sandstone Formation present in the southern part of the Danish area contains Variscan-aged zircon grains, which were transported across the North German Basin from the Variscan massifs by aeolian processes in this arid Early Triassic climate [61]. However, the Bunter Sandstone Formation contains other age populations that are not prominent in the southeastern part of the Gassum Formation, so reworking the Bunter Sandstone Formation cannot explain the entire zircon age distribution. The very prominent c. 1.65 Ga zircon age population found in all samples from the southeastern part of the Gassum Formation is not discernable in the Bunter Sandstone Formation since erosion of the Caledonian Orogen was not yet a prominent sediment source to the Danish area in the Early Triassic.

The basement and its sedimentary cover of the Ringkøbing–Fyn High can only have been eroded in limited amounts during deposition of the Gassum Formation, as indicated by interpretation of the available seismic data [15]. Furthermore, the age of its basement is comparable to the Telemarkia Terrane [39] so it cannot have supplied much material to the southeastern part of the basin. The content of angular rock fragments identified in the Sønderborg-1 well is then presumed to be a local occurrence of mixing with basement detritus eroded from the Ringkøbing–Fyn High. In parts of the Skurup High, Cretaceous sediments rest directly on crystalline basement of assumed Sveconorwegian affinity, so Triassic or Permian sediments perhaps containing Variscan-aged zircon grains may have been exposed to erosion during deposition of the Gassum Formation. Alternatively, the Skurup High functioned as a by-pass area for sediment eroded from the Variscan Orogen or its derived sediments, which would then have been transported northwards by fluvial processes.

The sediment supplied to the Gassum Formation cannot have been reworked from Fennoscandia-derived older sedimentary rocks such as Cambrian and Devonian since the zircon age populations do not match [39,62,63]. Reworking of the German Triassic Buntsandstein Group deposited north of the Variscan massifs is a likely source of the Variscan-aged zircon grains found in the Gassum Formation, possibly combined with sediment eroded from the highs at the time. The zircon ages in the Buntsandstein comprise first-cycle Carboniferous magmatic zircon grains besides Ediacaran to Paleozoic zircon grains reworked from metasediments and Gondwana-derived zircon grains with ages of c. 2 Ga [62]. These are comparable to age populations that are present in the SE Lower and Upper groups, but are absent in the NW Lower and Upper groups (Figure 6). A further indication of sediment supply from reworking of the Buntsandstein Group comprises Fe-oxide/hydroxide coatings on grains overgrown by quartz, rounded during transport (Figure 7). Such grains are found in the southeastern part of the Gassum Formation and

proves that these grains were supplied from the reworking of sediments deposited during an arid climate such as the Buntsandstein.

A contour map of the Variscan input to the Gassum Formation is produced based on a qualitative estimation of the relative content found in each sample (Figure 10). All 12 samples from the eight southernmost sampled wells have high Variscan input relative to the other samples. Thus, the Variscan zircon grains must have been supplied to the Danish area from the south or southeast, which is in agreement with their source area in the Variscan Orogen present in Central Europe. The Variscan input decreases to a medium to low relative amount in the samples from northern Sjælland and Kattegat. In Jylland, Variscan input is only distinct in the upper sample from the Horsens-1 well, so it appears that the deposition of Variscan sediment spread to a wider area extending further towards the west during the deposition of the upper part of the Gassum Formation. Variscan input has not been found in the samples from the 11 remaining wells, which are present farthest to the northwest with the Voldum-1 well being the most southeasterly. Based on the distribution of Variscan zircon grains in the Gassum Formation, it seems likely that sediment was transported from the southeast across the Skurup High and that sediment was supplied from the south simultaneously (Figure 10).

It is unlikely that the Variscan sediment could be transported as far north as the Skagerrak–Kattegat Platform area, so the Sorgenfrei–Tornquist Zone may be the northern limit of the sediment derived from the south (Figure 10). It cannot be determined how far to the west the Variscan sediment spread across southern Jylland since the Gassum Formation is mostly missing here, due to Middle Jurassic erosion. In eastern Denmark, the large sediment supply from the north diluted the smaller sediment supply from the south, which decreased in a northerly direction. However, the amount of Variscan sediment may be underestimated since Variscan ages are overrepresented both among the discordant ages and among those with common lead content, so it is possible that the amount of sediment supplied from the southeast may have been as large or even larger than the amount supplied from the north. The zircon fertility of the Variscan source rocks is not known so the content of Variscan versus Caledonian zircon grains cannot give a precise estimate of how large a proportion of the sediment was supplied from each source area. Furthermore, some fractionation between zircon and other mineral grains may have occurred during the sediment transport.

The fluvial system that transported sediment from the Caledonian Orogen to the Norwegian–Danish Basin must have been of a substantial size to be able to transport such a large amount of sediment to the basin and further south into the North German Basin. The sediment must have been produced by the pronounced Triassic exhumation of southern Norway where a succession of several kilometers of thickness was eroded away [55,64]. Renewed uplift may have occurred during the deposition of the Gassum Formation, which would explain why the sediment from the Caledonian Orogen began spreading to the entire Norwegian–Danish Basin instead of only the eastern part. The presumed tectonic movements in the hinterland occurred during the basin-wide regression associated with SB 5, which may thus be related to the uplift. The provenance signal of the sediments supplied to the Norwegian–Danish Basin seems to have changed permanently after this event, since the marked 1.65 Ga zircon age population from the Caledonian Orogen is not found in older Cambrian, Permian, and Triassic sediments [39,61,65]. On the contrary, this age population is dominant in Miocene sediments with zircon age distributions comparable to the upper part of the Gassum Formation [66] and the age population is also evident in sediment from the Ljungan river that drains the Caledonian nappes eastwards today [67].

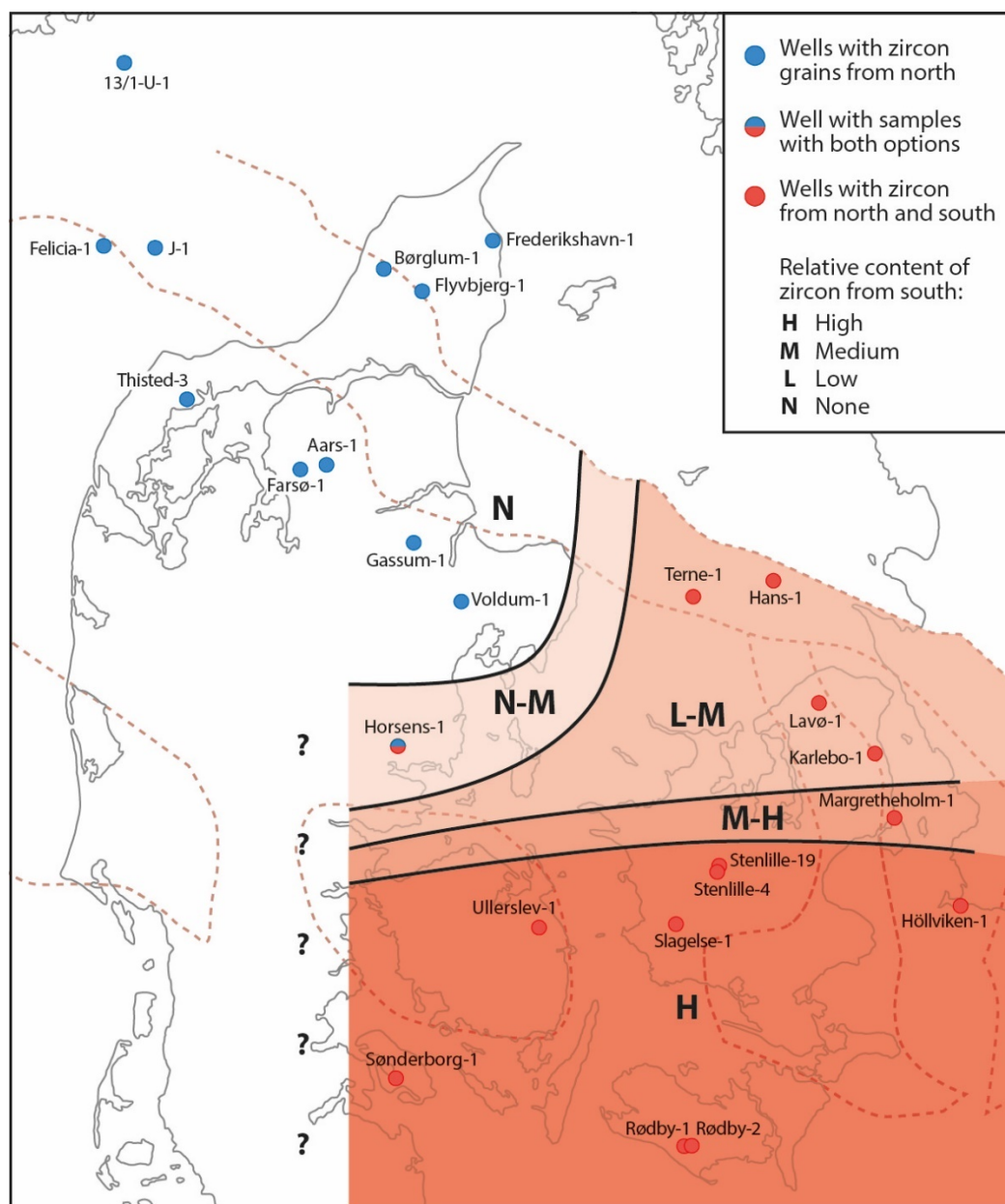


**Figure 10.** Contour map of the content of Variscan zircon grains in the Gassum Formation. The relative content of Variscan zircon grains in each sample has been classified as high, medium, low or none based on a qualitative estimation. Only one of the three samples from the Horsens-1 well contains Variscan zircon grains. It is evident that the zircon grains with Variscan ages have been supplied from the south or southeast, which is in accordance with the direction to the Variscan Orogen.

The provenance of the lower and upper parts of the Gassum Formation are summarized in Figure 11. The upper part of the figure shows the known extent of sediment supplied from each of the appointed sediment source areas, and the lower part shows the tentative paleogeographic reconstructions based on these results. The provenance divides indicated in the figure in the basin area delimit the extent of the sinks, and the location of the provenance divides changes between the lower and upper part of the formation. The rivers draining the Caledonian and Variscan Orogens presumably met east of the study area and supplied sediment of mixed composition into the basin, which is in accordance with the terrestrial deposition that took place east-southeast of the basin [68,69].

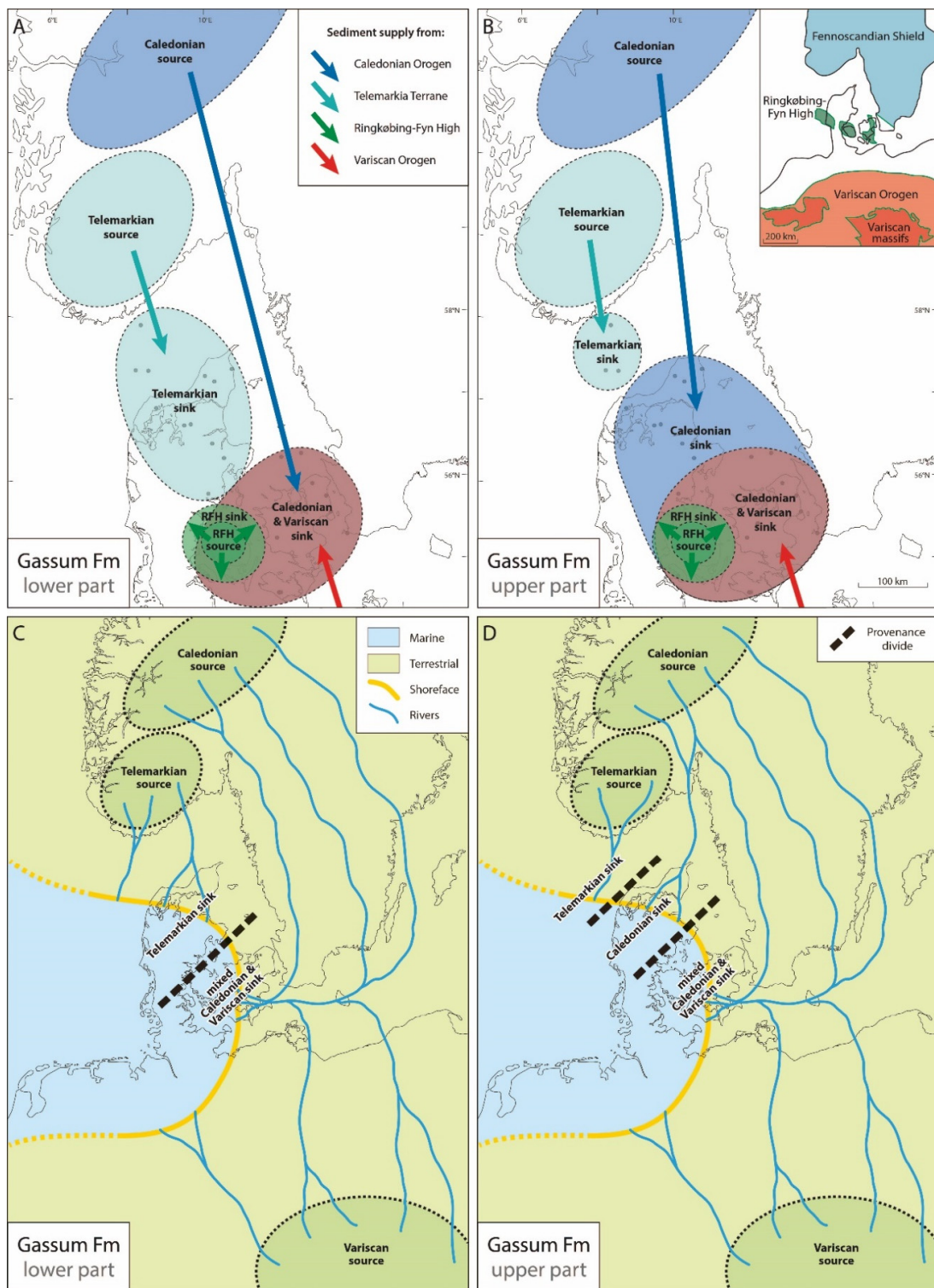


**Figure 11.** Provenance of the lower (A) and upper (B) parts of the Gassum Formation showing the location of the primary source areas (Caledonian, Sveconorwegian, and Variscan) and the minimum extend of their sinks as evident from zircon U-Pb data from wells in the Norwegian–Danish Basin and the northern North German Basin. Sediment was locally supplied from exposed parts of the Ringkøbing–Fyn High. Tentative paleogeographic reconstructions of these scenarios are shown for the lower (C) and upper (D) parts of the formation, where the primary difference is which of the Fennoscandian source areas that supplied most sediment to the basin. They represent snapshots since the coastline moved back and forth due repeated transgressions and regressions.

## 7. Conclusions

Zircon U-Pb data from the Upper Triassic–Lower Jurassic Gassum Formation sandstones, deposited in the Norwegian–Danish Basin, show that the dominant provenance is the Fennoscandian Shield in Scandinavia besides sediment contributions from the Variscan Orogen in Central Europe. The latter contribution only reached the southern part of the basin.

During deposition of the lower part of the Gassum Formation below the regional SB 5 surface, sediment with relatively low mineralogical maturity was deposited in the north-western part of the basin supplied from a local source area in the Telemarkia Terrane. At the same time, sediment with high mineralogical maturity was deposited in the southeastern part of the basin, which had been transported southwards from the Caledonian Orogen and northwards from the Variscan Orogen. When the upper part of the Gassum Formation overlying SB 5 was deposited, the sediment supply from the Caledonian Orogen spread to the entire basin, except in the Skagerrak area, where sediment was still supplied from the Telemarkia Terrane. The sediment from the Variscan Orogen also became distributed in a larger area extending further to the west.

The long transport distance from the Caledonian Orogen combined with the input of recycled sediments from the Variscan Orogen must have produced the high mineralogical maturity, indicating that intensive chemical weathering has occurred in the humid climate during temporary storage along the transport route, where the sediment was likely conveyed by large meandering rivers. The thoroughly homogenized zircon age populations and mineralogical compositions of the sandstones from the southeastern part of the Gassum Formation were presumably produced by mixing of fluvial supplies from the north and the south that merged east of the basin. The sediment from the Caledonian Orogen must be first-cycle since its dominant 1.65 Ga zircon age population was not supplied to the basin before this time, as evident in older sediments, whereas it is present in younger sediments. Thus, an uplift in the hinterland has likely occurred.

The provenance has major implications for the understanding of the distribution of sandstones in the basin and for the detrital mineralogical assemblage where the composition of the sediment source rock and the sediment transport distance is of importance combined with the time available for weathering. It is essential to consider the resulting large geographic and stratigraphic variations in mineralogical composition across the basin when predicting diagenesis and reservoir quality.

**Supplementary Materials:** The following supporting information can be downloaded at: <https://www.mdpi.com/article/10.3390/geosciences12080308/s1>.

**Author Contributions:** M.O. did the data interpretation and manuscript writing in cooperation with the other authors. H.V. and L.H.N. made the sequence stratigraphic correlations. R.W. and M.O. performed the petrographic work. S.N.M. made the mineral maps. B.D.H. and T.B.T. made the geochronological work. All authors have read and agreed to the published version of the manuscript.

**Funding:** The zircon U-Pb analyses of the Gassum Formation have been performed as part of several projects during the last decade and we would like to thank the following for funding: Innovation Fund Denmark, the Danish Council for Strategic Research, the Research Council of Norway, CLIMIT, APMH, HOFOR, and EUDP.

**Institutional Review Board Statement:** Not applicable.

**Informed Consent Statement:** Not applicable.

**Data Availability Statement:** Not applicable.

**Acknowledgments:** The zircon U-Pb analyses of the Gassum Formation have been performed as part of several projects during the last decade and we would like to thank the following for funding: Innovation Fund Denmark, the Danish Council for Strategic Research, the Research Council of Norway, CLIMIT, APMH, HOFOR, and EUDP. NPD and SINTEF (Atle Mørk) and SGU (Mikael Erlström) are thanked for permission to sample the 13/1-U-1 and Höllviken-1 wells, respectively. Mojagan Alaei, Simon H. Serre, Fiorella F. Aguilera, Michael S. Nielsen, Olga Nielsen, Lisbeth L. Nielsen and Marga Jørgensen are thanked for careful sample preparation and analysis. Jette Halskov and Carsten E. Thuesen are thanked for artwork and Catherine Jex for language polishing. Finally, the authors would like to thank the reviewers for their valuable advice that helped improve the manuscript.

**Conflicts of Interest:** The authors declare no conflict of interest.

## References

1. Avigad, D.; Sandler, A.; Kolodner, K.; Stern, R.J.; McWilliams, M.; Miller, N.; Beyth, M. Mass-production of Cambro–Ordovician quartz-rich sandstone as a consequence of chemical weathering of Pan-African terranes: Environmental implications. *Earth Planet. Sci. Lett.* **2005**, *240*, 818–826. [\[CrossRef\]](#)
2. Garzanti, E. The maturity myth in sedimentology and provenance analysis. *J. Sediment. Res.* **2017**, *87*, 353–365. [\[CrossRef\]](#)
3. Lorentzen, S.; Augustsson, C.; Nystuen, J.P.; Berndt, J.; Jahren, J.; Schovsbo, N.H. Provenance and sedimentary processes controlling the formation of lower Cambrian quartz arenite along the southwestern margin of Baltica. *Sediment. Geol.* **2018**, *375*, 203–217. [\[CrossRef\]](#)
4. Nauton-Fourteu, M.; Tyrrell, S.; Morton, A.; Mark, C.; O’Sullivan, G.J.; Chew, D.M. Constraining recycled detritus in quartz-rich sandstones: Insights from a multi-proxy provenance study of the Mid-Carboniferous, Clare Basin, western Ireland. *Basin Res.* **2021**, *33*, 342–363. [\[CrossRef\]](#)
5. Weibel, R.; Olivarius, M.; Kristensen, L.; Friis, H.; Hjuler, M.L.; Kjølner, C.; Mathiesen, A.; Nielsen, L.H. Predicting permeability of low-enthalpy geothermal reservoirs: A case study from the Upper Triassic—Lower Jurassic Gassum Formation, Norwegian–Danish Basin. *Geothermics* **2017**, *65*, 135–157. [\[CrossRef\]](#)
6. Kristensen, L.; Hjuler, M.L.; Frykman, P.; Olivarius, M.; Weibel, R.; Nielsen, L.H.; Mathiesen, A. Pre-drilling assessments of average porosity and permeability in the geothermal reservoirs of the Danish area. *Geotherm. Energy* **2016**, *4*, 6. [\[CrossRef\]](#)
7. Andersen, O.; Sundal, A. Estimating Caprock Impact on CO<sub>2</sub> Migration in the Gassum Formation Using 2D Seismic Line Data. *Trans. Porous Med.* **2021**, *138*, 459–487. [\[CrossRef\]](#)
8. Bredesen, K. Assessing rock physics and seismic characteristics of the Gassum Formation in the Stenlille aquifer gas storage—A reservoir analog for the Havnsø CO<sub>2</sub> storage prospect, Denmark. *Int. J. Greenh. Gas. Control* **2022**, *114*, 103583. [\[CrossRef\]](#)
9. Chopra, S.; Sharma, R.K.; Bredesen, K.; Marfurt, K.J. Seismic reservoir characterization of the Gassum Formation in the Stenlille aquifer gas storage, Denmark: Part-1. *Interpretation* **2022**, *10*, 1–55. [\[CrossRef\]](#)
10. Frykman, P.; Nielsen, L.H.; Vangkilde-Petersen, T.; Anthonsen, K. The potential for large-scale, subsurface geological CO<sub>2</sub> storage in Denmark. *Geol. Surv. Den. Greenl. Bull.* **2009**, *17*, 13–16. [\[CrossRef\]](#)
11. Mathiesen, A.; Nielsen, L.H.; Bidstrup, T. Identification of the potential geothermal reservoirs in Denmark. *Geol. Surv. Den. Greenl. Bull.* **2010**, *20*, 19–22.
12. Mathiesen, A.; Nielsen, L.H.; Vosgerau, H.; Poulsen, S.E.; Bjørn, H.; Røgen, B.; Ditlefsen, C.; Vangkilde-Pedersen, T. *Geothermal Energy Use, Country Update Report for Denmark*; Proceedings World Geothermal Congress: Reykjavik, Iceland, 2020; 14p.
13. Nielsen, L.H.; Japsen, P. Deep wells in Denmark 1935–1900. Lithostratigrafisk subdivision. *Geol. Surv. Den. Ser. A* **1991**, *31*, 179.
14. Pasquinelli, L.; Felder, M.; Gulbrandsen, M.L.; Hansen, T.M.; Jeon, J.-S.; Molenaar, N.; Mosegaard, K.; Fabricius, I.L. The feasibility of high-temperature aquifer thermal energy storage in Denmark: The Gassum Formation in the Stenlille structure. *Bull. Geol. Soc. Den.* **2020**, *68*, 133–154. [\[CrossRef\]](#)
15. Vosgerau, H.; Mathiesen, A.; Andersen, M.S.; Boldreel, L.O.; Hjuler, M.L.; Kamla, E.; Kristensen, L.; Pedersen, K.B.; Pjetursson, B.; Nielsen, L.H. A WebGis portal for exploration of deep geothermal energy based on geological and geophysical data. *Geol. Surv. Den. Greenl. Bull.* **2016**, *35*, 23–26. [\[CrossRef\]](#)
16. Weibel, R.; Olivarius, M.; Vosgerau, H.; Mathiesen, A.; Kristensen, L.; Nielsen, C.M.; Nielsen, L.H. Overview of potential geothermal reservoirs in Denmark. *Neth. J. Geosci.* **2020**, *99*, 14. [\[CrossRef\]](#)
17. Morton, A.C.; Hallsworth, C.R. Processes controlling the composition of heavy mineral assemblages in sandstones. *Sediment. Geol.* **1999**, *124*, 3–29. [\[CrossRef\]](#)
18. Andersen, T.; Elburg, M.A.; Magwaza, B.N. Sources of bias in detrital zircon geochronology: Discordance, concealed lead loss and common lead correction. *Earth-Sci. Rev.* **2019**, *197*, 102899. [\[CrossRef\]](#)
19. Herrmann, M.; Söderlund, U.; Scherstén, A.; Næraa, T.; Holm-Alwmark, S.; Alwmark, C. The effect of low-temperature annealing on discordance of U–Pb zircon ages. *Sci. Rep.* **2021**, *11*, 7079. [\[CrossRef\]](#)
20. Weibel, R.; Olivarius, M.; Kjølner, C.; Kristensen, L.; Hjuler, M.L.; Friis, H.; Pedersen, P.K.; Boyce, A.; Andersen, M.S.; Kamla, E.; et al. The influence of climate on early and burial diagenesis of Triassic and Jurassic sandstones from the Norwegian–Danish Basin. *Depos. Rec.* **2017**, *3*, 60–91. [\[CrossRef\]](#)

21. Larsen, G. Rhaetic-Jurassic-Lower Cretaceous sediments in the Danish Embayment (a heavy-mineral study). *Geol. Surv. Den. Row* **2** **1966**, *91*, 1–127.
22. Bertelsen, F. The Upper Triassic–Lower Jurassic Vinding and Gassum formations of the Norwegian-Danish Basin. *Geol. Surv. Den. Ser. B* **1978**, *3*, 1–26. [[CrossRef](#)]
23. Michelsen, O.; Nielsen, L.H.; Johannessen, P.N.; Andsbjerg, J.; Surlyk, F. Jurassic lithostratigraphy and stratigraphic development onshore and offshore Denmark. *Geol. Surv. Den. Greenl. Bull.* **2003**, *1*, 147–216.
24. Nielsen, L.H. Late Triassic–Jurassic development of the Danish Basin and Fennoscandian Border Zone, Southern Scandinavia. *Geol. Surv. Den. Greenl. Bull.* **2003**, *1*, 459–526.
25. Vejrbæk, O.V. Dybe strukturer i danske sedimentære bassiner. *Geol. Tidsskr.* **1997**, *4*, 1–31.
26. Michelsen, O.; Clausen, O.R. Detailed stratigraphic subdivision and regional correlation of the southern Danish Triassic succession. *Mar. Pet. Geol.* **2002**, *19*, 563–587. [[CrossRef](#)]
27. Japsen, P.; Green, P.F.; Nielsen, L.H.; Rasmussen, E.S.; Bidstrup, T. Mesozoic–Cenozoic exhumation events in the eastern North Sea Basin: A multi-disciplinary study based on palaeothermal, palaeoburial, stratigraphic and seismic data. *Basin Res.* **2007**, *19*, 451–490. [[CrossRef](#)]
28. Bingen, B.; Solli, A. Geochronology of magmatism in the Caledonian and Sveconorwegian belts of Baltica: Synopsis for detrital zircon provenance studies. *Nor. J. Geol.* **2009**, *89*, 267–290.
29. Bingen, B.; Nordgulen, Ø.; Viola, G. A four-phase model for the Sveconorwegian orogeny, SW Scandinavia. *Nor. J. Geol.* **2008**, *88*, 43–72.
30. Heeremans, M.; Faleide, J.I. Late Carboniferous–Permian tectonics and magmatic activity in the Skagerrak, Kattegat and the North Sea. *Geol. Soc. Lond. Spec. Publ.* **2004**, *223*, 157–176. [[CrossRef](#)]
31. Breitzkreuz, C.; Kennedy, A. Magmatic flare-up at the Carboniferous/Permian boundary in the NE German Basin revealed by SHRIMP zircon ages. *Tectonophysics* **1999**, *302*, 307–326. [[CrossRef](#)]
32. Anthes, G.; Reischmann, T. Timing of granitoid magmatism in the eastern mid-German crystalline rise. *J. Geodyn.* **2001**, *31*, 119–143. [[CrossRef](#)]
33. Erlström, M.; Sivhed, U. Pre-Rhaetian Triassic strata in Scania and adjacent offshore areas—stratigraphy, petrology and subsurface characteristics. *Geol. Surv. Swed. Rapp. Och Medd.* **2012**, *132*, 74.
34. Jarsve, E.M.; Maast, T.E.; Gabrielsen, R.H.; Faleide, J.I.; Nystuen, J.P.; Sassier, C. Seismic stratigraphic subdivision of the Triassic succession in the Central North Sea; integrating seismic reflection and well data. *J. Geol. Soc. Lond.* **2014**, *171*, 353–374. [[CrossRef](#)]
35. Vejrbæk, O.V.; Britze, P. Geological map of Denmark 1:750,000. Top pre-Zechstein (two-way travelttime and depth). *Geol. Surv. Den. Map Ser.* **1994**, *45*, 8.
36. Lassen, A.; Thybo, H. Neoproterozoic and Palaeozoic evolution of SW Scandinavia based on integrated seismic interpretation. *Precambrian Res.* **2012**, *204–205*, 75–104. [[CrossRef](#)]
37. Lahtinen, R.; Garde, A.A.; Melezhik, V.A. Paleoproterozoic evolution of Fennoscandia and Greenland. *Episodes* **2008**, *31*, 20–28. [[CrossRef](#)]
38. Waight, T.E.; Frei, D.; Storey, M. Geochronological constraints on granitic magmatism, deformation, cooling and uplift on Bornholm, Denmark. *Bull. Geol. Soc. Den.* **2012**, *60*, 23–46.
39. Olivarius, M.; Friis, H.; Kokfelt, T.F.; Wilson, J.R. Proterozoic basement and Paleozoic sediments in the Ringkøbing-Fyn High characterized by zircon U–Pb ages and heavy minerals from Danish onshore wells. *Bull. Geol. Soc. Den.* **2015**, *63*, 29–44.
40. Olivarius, M.; Sundal, A.; Weibel, R.; Gregersen, U.; Baig, I.; Thomsen, T.B.; Kristensen, L.; Hellevang, H.; Nielsen, L.H. Provenance and sediment maturity as controls on CO<sub>2</sub> mineral sequestration potential of the Gassum Formation in the Skagerrak. *Front. Earth Sci.* **2019**, *7*, 23. [[CrossRef](#)]
41. Jackson, S.E.; Pearson, N.J.; Griffin, W.L.; Belousova, E.A. The application of laser ablation-inductively coupled plasma-mass spectrometry to in situ U–Pb zircon geochronology. *Chem. Geol.* **2004**, *211*, 47–69. [[CrossRef](#)]
42. Slama, J.; Kosler, J.; Condon, D.J.; Crowley, J.L.; Gerdes, A.; Hanchar, J.M.; Horstwood, S.A.; Morris, G.A.; Nasdala, L.; Norberg, N.; et al. Plesovice zircon—a new natural reference material for U–Pb and Hf isotopic microanalysis. *Chem. Geol.* **2008**, *249*, 1–35. [[CrossRef](#)]
43. Wiedenbeck, M.; Allé, P.; Corfu, F.; Griffin, W.L.; Meier, M.; Oberli, F.; von Quadt, A.; Roddick, J.C.; Spiegel, W. Three natural zircon standards for U–Th–Pb, Lu–Hf, trace element and REE analyses. *Geostand. Newsl.* **1995**, *19*, 1–23. [[CrossRef](#)]
44. Wiedenbeck, M.; Hanchar, J.M.; Peck, W.H.; Sylvester, P.; Valley, J.; Whitehouse, M.; Kronz, A.; Morishita, Y.; Nasdala, L.; Fiebig, J.; et al. Further characterisation of the 91,500 zircon crystal. *Geostand. Geoanalytical Res.* **2004**, *28*, 9–39. [[CrossRef](#)]
45. Hellström, J.; Paton, C.; Woodhead, J.; Hergt, J. Iolite: Software for spatially resolved LA- (quad and MC) ICPMS analysis. In *Laser Ablation ICP–MS in the Earth Sciences: Current Practices and Outstanding Issues*; Sylvester, P., Ed.; Mineralogical Association of Canada Short Course: Vancouver, BC, Canada, 2008; pp. 343–348.
46. Paton, C.; Hellstrom, J.C.; Paul, P.; Woodhead, J.D.; Hergt, J.M. Iolite: Freeware for the visualisation and processing of mass spectrometric data. *J. Anal. At. Spectrom.* **2011**, *26*, 2508–2518. [[CrossRef](#)]
47. Petrus, J.A.; Kamber, B.S. VizualAge: A novel approach to laser ablation ICP–MS U–Pb geochronology data reduction. *Geostand. Geoanalytical Res.* **2012**, *36*, 247–270. [[CrossRef](#)]
48. Thomsen, T.B.; Heijboer, T.; Guarnieri, P. jAgeDisplay: Software for evaluation of data distributions in U–Th–Pb geochronology. *Geol. Surv. Den. Greenl. Bull.* **2016**, *35*, 103–106. [[CrossRef](#)]
49. Wetherill, G.W. Discordant Uranium–Lead Ages, I. *Trans. Am. Geophys. Union* **1956**, *37*, 320–326. [[CrossRef](#)]

50. Gehrels, G. Detrital zircon U-Pb geochronology: Current methods and new opportunities. In *Tectonics of Sedimentary Basins: Recent Advances*; Busby, C., Azor, A., Eds.; Wiley Online Library: Hoboken, NJ, USA, 2011.
51. Keulen, N.; Malkki, S.N.; Graham, S. Automated quantitative mineralogy applied to metamorphic rocks. *Minerals* **2020**, *10*, 47. [[CrossRef](#)]
52. Japsen, P.; Bidstrup, T. Quantification of late Cenozoic erosion in Denmark based on sonic data and basin modelling. *Bull. Geol. Soc. Den.* **1999**, *46*, 79–99. [[CrossRef](#)]
53. Bertelsen, F. Lithostratigraphy and depositional history of the Danish Triassic. *Geol. Surv. Den. Ser. B* **1980**, *4*, 59. [[CrossRef](#)]
54. Lidmar-Bergström, K. Denudation surfaces and tectonics in the southernmost part of the Baltic Shield. *Precambrian Res.* **1993**, *64*, 337–345. [[CrossRef](#)]
55. Japsen, P.; Green, P.F.; Bonow, J.M.; Erlström, M. Episodic burial and exhumation of the southern Baltic Shield: Epeirogenic uplifts during and after break-up of Pangaea. *Gondwana Res.* **2016**, *35*, 357–377. [[CrossRef](#)]
56. Andersen, T.; Saeed, A.; Gabrielsen, R.H.; Olausson, S. Provenance characteristics of the Brumunddal sandstone in the Oslo Rift derived from U-Pb, Lu-Hf and trace element analyses of detrital zircons by laser ablation ICMPS. *Nor. J. Geol.* **2011**, *91*, 1–19.
57. Dahlgren, S.; Corfu, F. Northward sediment transport from the late Carboniferous Variscan Mountains: Zircon evidence from the Oslo Rift, Norway. *J. Geol. Soc. Lond.* **2001**, *158*, 29–36. [[CrossRef](#)]
58. Kristoffersen, M.; Andersen, T.; Andresen, A. U-Pb age and Lu-Hf signatures of detrital zircon from Palaeozoic sandstones in the Oslo Rift, Norway. *Geol. Mag.* **2014**, *151*, 816–829. [[CrossRef](#)]
59. Slama, J. Rare late Neoproterozoic detritus in SW Scandinavia as a response to distant tectonic processes. *Terra Nova* **2016**, *28*, 394–401. [[CrossRef](#)]
60. White, A.F.; Bullen, T.D.; Schulz, M.S.; Blum, A.E.; Huntington, T.G.; Peters, N.E. Differential rates of feldspar weathering in granitic regoliths. *Geochim. Et Cosmochim. Acta* **2001**, *65*, 847–869. [[CrossRef](#)]
61. Olivarius, M.; Weibel, R.; Friis, H.; Boldreel, L.O.; Keulen, N.; Thomsen, T.B. Provenance of the Lower Triassic Bunter Sandstone Formation: Implications for distribution and architecture of aeolian vs. fluvial reservoirs in the North German Basin. *Basin Res.* **2017**, *29*, 113–130. [[CrossRef](#)]
62. Augustsson, C.; Voigt, T.; Bernhart, K.; Kreißler, M.; Gaupp, R.; Gärtner, A.; Hofmann, M.; Linnemann, U. Zircon size-age sorting and source-area effect: The German Triassic Buntsandstein Group. *Sediment. Geol.* **2018**, *375*, 218–231. [[CrossRef](#)]
63. Franke, W.; Dulce, J.-C. Back to sender: Tectonic accretion and recycling of Baltica-derived Devonian clastic sediments in the Rheno-Hercynian Variscides. *Int. J. Earth Sci. (Geol. Rundsch.)* **2017**, *106*, 377–386. [[CrossRef](#)]
64. Rohrman, M.; van der Beek, P.; Andriessen, P.; Cloeting, S. Meso-Cenozoic morphotectonic evolution of southern Norway: Neogene domal uplift inferred from apatite fission track thermochronology. *Tectonics* **1995**, *14*, 704–718. [[CrossRef](#)]
65. Olivarius, M.; Nielsen, L.H. Triassic paleogeography of the greater eastern Norwegian-Danish Basin: Constraints from provenance analysis of the Skagerrak Formation. *Mar. Pet. Geol.* **2016**, *69*, 168–182. [[CrossRef](#)]
66. Olivarius, M.; Rasmussen, E.S.; Siersma, V.; Knudsen, C.; Kokfelt, T.F.; Keulen, N. Provenance signal variations caused by facies and tectonics: Zircon age and heavy mineral evidence from Miocene sand in the north-eastern North Sea Basin. *Mar. Pet. Geol.* **2014**, *49*, 1–14. [[CrossRef](#)]
67. Morton, A.; Fanning, M.; Milner, P. Provenance characteristics of Scandinavian basement terrains: Constraints from detrital zircon ages in modern river sediments. *Sediment. Geol.* **2008**, *210*, 61–85. [[CrossRef](#)]
68. Barth, G.; Franz, M.; Heunisch, C.; Ernst, W.; Zimmermann, J.; Wolfgramm, M. Marine and terrestrial sedimentation across the T-J transition in the North German Basin. *Palaeogeogr. Palaeoclimatol. Palaeoecol.* **2018**, *489*, 74–94. [[CrossRef](#)]
69. Barth, G.; Pienkowski, G.; Zimmermann, J.; Franz, M.; Khulman, G. Palaeogeographical evolution of the Lower Jurassic: High-resolution biostratigraphy and sequence stratigraphy in the Central European Basin. *Geol. Soc. Lond. Spec. Publ.* **2018**, *469*, 341. [[CrossRef](#)]